Proceedings of the
44th IEEE Conference on Decision and Control, and
the European Control Conference 2005
Seville, Spain, December 12-15, 2005

Drag-Free and Attitude Control for the GOCE satellite

Davide Andreis, Enrico S. Canuto, *Member IEEE*

***Abstract*—The paper concerns Drag-Free and Attitude Control (DFAC) of the European satellite GOCE to be employed during scientific mission phase. DFAC has been designed and tested on the end-to-end GOCE simulator. The design has followed the Embedded Model Control methodology, where a spacecraft/environment discrete-time model (embedded model) becomes the real-time core of the DFAC and is interfaced to the plant via tunable command and measurement laws. Simulation results are presented.**

I. Introduction

THE scientific goal of the European space mission Gravity Field and Steady-state Ocean Circulation Explorer (GOCE) is the recovery of the stationary Earth's gravity field anomalies down to 1mGal (=10 μm/s^2) and of geoid heights down to 1cm over the Earth's surface at a spatial resolution better than 100 km [3].

The traditional techniques of gravity field determination have reached their intrinsic limits [1]. Any advances must rely on space techniques. To this end, GOCE will implement three main concepts:

1) *Precise orbit determination* by satellite-to-satellite tracking. The orbit of a Low Earth satellite can be monitored to cm-precision by means of a GPS receiver. Such techniques are limited by progressive attenuation of the gravity field at satellite altitudes.
2) *Satellite gravity gradiometry*. An on-board Gravity Gradiometer (GG) measures the components of the gravity gradient tensor $\mathbf{U} = \nabla^2 U$ exploiting a differential approach for enlightening the effect of small-scale features, corresponding to the mission Measurement Bandwidth (MBW):

$$\mathcal{F}_1 = \{ f_1 = 0.005 \le f \le f_2 = 0.1 \text{ Hz} \}, \qquad (1)$$

   i.e. the frequency region where the measurement accuracy of $\mathbf{U}$ has to be maximized.
3) *Drag-Free and Attitude Control* (DFAC). To extract gravity field from orbit and GG measurements, non-gravitational forces must be compensated by a drag-free control mechanism and the spacecraft attitude must be accurately aligned to the *Local Orbital Reference Frame* $\mathcal{R}_O$ (LORF), to which gravity gradient measurements will be referred.

The GOCE satellite will fly on a near-circular sun-synchronous, quasi-polar orbit at a mean altitude $h \cong 250$ km, matching the orbital rate $\omega_O \approx 1.17 \cdot 10^{-3}$ s^{-1}. The launch is planned to take place in 2006 and the overall mission will last at least 20 months.

The paper outlines the design and the simulated results of the DFAC, active during commissioning and scientific mission phases. The design has followed the Embedded Model Control (EMC) methodology (see [4]–[6]). The main reference frames and the DFAC requirements are presented in section II. The fine model is briefly described in section III, paying attention to disturbance, sensor and actuator dynamics. Section IV introduces the EM and section V gives an overview of the relevant digital control. Simulated results are provided in section VI.

II. Reference frames and DFAC requirements

The main GOCE reference frame is the so-called Local Orbital Reference Frame (LORF) $\mathcal{R}_O = \{C, \mathbf{i}_O, \mathbf{j}_O, \mathbf{k}_O\}$, which defines the instantaneous spacecraft orbit orientation, and specifically (i) the Centre-of-Mass (COM) direction aligned with the inertial velocity $\mathbf{v}$ and (ii) the orbital plane orthogonal to the angular momentum $\mathbf{h} = m\mathbf{r} \times \mathbf{v}$, where $m \simeq 1000$ kg is the spacecraft mass and $\mathbf{r}$ the COM position. The origin C is the satellite COM and the axes are defined by:

$$\mathbf{i}_O = \mathbf{v} / \|\mathbf{v}\|, \mathbf{j}_O = \mathbf{r} \times \mathbf{v} / \|\mathbf{r} \times \mathbf{v}\|, \mathbf{k}_O = \mathbf{i}_O \times \mathbf{j}_O . \qquad (2)$$

The matrix $\mathbf{R}_O(\mathbf{r}, \mathbf{v}) = [\mathbf{i}_O \quad \mathbf{j}_O \quad \mathbf{k}_O]$, i.e. the LORF-to-inertial coordinates transformation, defines the reference quaternion $\mathcal{Q}_O$ to be tracked by the spacecraft attitude quaternion $\mathcal{Q}$ during mission.

The body frame, or *Attitude Control Reference Frame* (ACRF) $\mathcal{R} = \{C, \mathbf{i}, \mathbf{j}, \mathbf{k}\}$, is imposed by geometry and mass distribution of the spacecraft, which is a slender cylindrical body. The ACRF unit vectors are aligned with the principal axes of inertia and $\mathbf{i}$, aligned with the cylinder axis, points

This work has been in part supported by a grant from Alenia Spazio, prime contractor of GOCE satellite.

E. S. Canuto is with Politecnico di Torino, Dipartimento di Automatica e Informatica, Corso Duca degli Abruzzi 24, 10129, Torino, Italy. (Corresponding author: Phone: +39-011-564-7026; Fax: +39-011-564-7099; e-mail: enrico.canuto@polito.it).

D. Andreis is with Politecnico di Torino, Dipartimento di Automatica e Informatica (e-mail: davide.andreis@polito.it).

toward $\mathbf{v}$. Modelling and control design assumes DFAC to keep the inertial attitude quaternion $\mathcal{Q}$ aligned with the reference quaternion $\mathcal{Q}_O$. Accordingly, the attitude vector $\mathbf{q}=\{q_x,q_y,q_z\}$ can be defined as the Euler angles entering the body-to-LORF transformation

$$\mathbf{R}(\mathbf{q})=\mathbf{Z}(q_z)\mathbf{Y}(q_y)\mathbf{X}(q_x), \qquad (3)$$

where $\mathbf{X}(q_x)$, $\mathbf{Y}(q_y)$ and $\mathbf{Z}(q_z)$ denote usual roll, pitch and yaw rotations matrices.

DFAC requirements are defined in terms of

1) the residual non-gravitational COM acceleration $\mathbf{a}$, in LORF coordinates, to be zeroed by drag-free control,
2) the satellite angular acceleration $\dot{\boldsymbol{\omega}}$,
3) the misalignment between ACRF and LORF expressed by the attitude $\mathbf{q}$ and the rate $\Delta\boldsymbol{\omega}=\omega_O\mathbf{j}_O-\mathbf{R}_O\boldsymbol{\omega}$, where $\boldsymbol{\omega}$ is the inertial angular rate and ω_O is the instantaneous orbit rate defined by

$$\omega_O=\|\mathbf{r}\times\mathbf{v}\|/\|\mathbf{r}\|^2. \qquad (4)$$

DFAC requirements (see TABLE 1) are not uniform within the control frequency band $\mathcal{F}_c$ from DC to $0.5f_c=0.5/T=5$ Hz, T being the DFAC time unit. Indeed, they are stringent in the MBW defined in (1) and relaxed at lower and higher frequencies, denoted as $\mathcal{F}_0=\{f\le f_1\}$ and $\mathcal{F}_2=\{f_2\le f\le f_c/2\}$, respectively.

TABLE 1
GOCE DRAG-FREE AND ATTITUDE CONTROL REQUIREMENTS

Var.	PSD (RMS) unit	$\mathcal{F}_0$	$\mathcal{F}_1$	$\mathcal{F}_2$
$\mathbf{a}$	$\mu m/\left(s^2\sqrt{Hz}\right)\left(\mu m/s^2\right)$	35 (0.5)	0.025	0.2
$\dot{\boldsymbol{\omega}}$	$\mu rad/\left(s^2\sqrt{Hz}\right)\left(\mu rad/s^2\right)$	70 (1)	0.025	0.025
$\Delta\boldsymbol{\omega}$	$\mu rad/\left(s\sqrt{Hz}\right)\left(\mu rad/s\right)$	700 (10)	0.5	NA
$\mathbf{q}$	$\mu rad/\sqrt{Hz}\left(\mu rad\right)$	26000 (370)	7.9	NA

In this paper PSD stands for root of unilateral Power Spectral Density.

III. FINE MODEL OF THE GOCE SATELLITE

The fine model accounts for: (i) spacecraft COM and attitude dynamics, (ii) perturbing forces and torques, (iii) actuator and sensor dynamics and noise.

A. 6-axes spacecraft dynamics

The 6-axes spacecraft dynamics is a standard one. The COM state equations, written in the $J2000$ Earth-centered inertial frame, are the following:

$$\begin{aligned}&\dot{\mathbf{r}}(t)=\mathbf{v}(t),\quad \mathbf{r}(t_0)=\mathbf{r}_0\\&\dot{\mathbf{v}}(t)=-\mathbf{R}_E\mathbf{g}(t)+\mathbf{R}_O(\mathbf{r},\mathbf{v})\mathbf{a}(t),\ \mathbf{v}(t_0)=\mathbf{v}_0\\&\mathbf{a}(t)=\left(\mathbf{F}_d(\mathbf{r},\mathbf{v},\mathbf{q},t)+\mathbf{R}(\mathbf{q})\mathbf{F}(t)\right)/m.\end{aligned} \qquad (5)$$

In (5), $\mathbf{g}=\nabla U(\mathbf{r}_E)$ is the gravity acceleration in Earth-fixed coordinates depending on the COM position $\mathbf{r}_E=\mathbf{R}_E^{-1}\mathbf{r}$, $\mathbf{R}_E$ is the Earth-fixed to inertial transformation, $\mathbf{F}_d$ is the LORF vector of the environment forces and $\mathbf{F}$ is the force actuated by thrusters, in body coordinates.

Attitude kinematics (6) is written in Euler angles by expressing the inertial rate $\boldsymbol{\omega}$ in LORF coordinates:

$$\mathbf{Z}(q_z)\mathbf{Y}(q_y)\begin{vmatrix}\dot{q}_x\\\dot{q}_y\\0\end{vmatrix}+\begin{vmatrix}0\\0\\\dot{q}_z\end{vmatrix}=\mathbf{R}(\mathbf{q})\boldsymbol{\omega}-\begin{vmatrix}0\\\omega_O\\0\end{vmatrix},\ \mathbf{q}(0)=\mathbf{q}_0. \qquad (6)$$

Attitude dynamics is a classical Euler equation:

$$\dot{\boldsymbol{\omega}}(t)=\mathbf{J}^{-1}\left(-\boldsymbol{\omega}(t)\times\mathbf{J}\boldsymbol{\omega}(t)+\mathbf{D}(t)+\mathbf{C}(t)\right),\boldsymbol{\omega}(0)=\boldsymbol{\omega}_0, \qquad (7)$$

where $\mathbf{J}$ is the inertia tensor, $\mathbf{D}$ is the vector of disturbance torques and $\mathbf{C}$ is the control torque vector.

B. Perturbing forces and torques

Three perturbations have prominent effects to GOCE motion: (i) gravity $\mathbf{g}$ and its anomalies determining the COM orbit and the gravity gradient torque $\mathbf{C}_g$, (ii) the drag force $\mathbf{F}_{drag}$ and torque $\mathbf{C}_{drag}$, (iii) the Earth magnetic field, which coupling with the spacecraft electrical dipole, yields the magnetic torque $\mathbf{C}_m$.

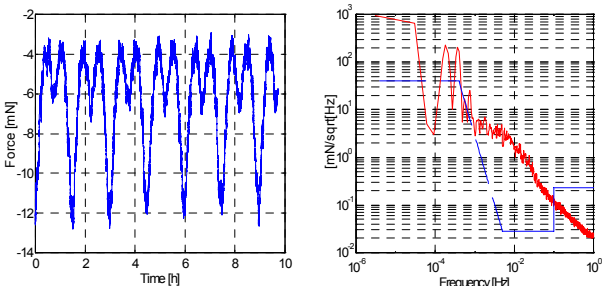

Fig. 1. The along-track drag. Left: time history (abscissas: hours, ordinates: mN). Right: PSD (ordinates: $mN/\sqrt{Hz}$) compared to acceleration requirement in force units (TABLE 1).

It is outside the paper's scope to deal with fine models of gravity, drag and magnetic perturbations (see [2] and [3]), as they are quite common. Instead, it is essential that they are accurate enough in the control bandwidth $\mathcal{F}_c$, to allow testing DFAC in a realistic way and synthesizing a robust stochastic class $\mathcal{D}$ of the unknown disturbances to be part of the EM. As an example, Fig. 1 shows time history and PSD of the along-track drag under worse solar activity.

C. Actuator dynamics and noise

DFAC requirements in TABLE 1 can only be met by employing suitable thrusters to actuate DFAC.

1) A pair of Ion Thrusters Assemblies (ITA), in cold redundancy, will counteract the along-track drag F_{dx} in a frequency band from DC to MBW.
2) Eight Micro-Thrusters Assemblies (MTA) will counteract cross-axis drag components F_{dy},F_{dz} and track the reference attitude. Presently, criticalities in MTA technology forced to abandon them in favour of a magnetic attitude control, implying DFAC requirements to be relaxed and lateral COM motion to be free.

Let V_t denote the voltage command of the active ITA

and $\mathbf{V}_m$ the voltage command of the MTA. By neglecting their dynamic response, a static voltage-to-acceleration relation may be written:

$$\begin{bmatrix}\mathbf{F}/m\\ \mathbf{J}^{-1}\mathbf{C}\end{bmatrix}=\mathbf{B}\left(\begin{bmatrix}K_tV_t\\ \mathbf{K}_m\mathbf{V}_m\end{bmatrix}+\begin{bmatrix}v_t\\ \mathbf{v}_m\end{bmatrix}\right),\ \begin{bmatrix}u_t\\ \mathbf{u}_m\end{bmatrix}=\begin{bmatrix}K_tV_t\\ \mathbf{K}_m\mathbf{V}_m\end{bmatrix}. \quad (8)$$

Notice that some of the entries in $\mathbf{B}$ in (8) are negligible, especially those coupling $\mathbf{V}_m$ to along-track acceleration F_x/m. Instead, ITA coupling to lateral accelerations F_y/m and F_z/m and to angular acceleration $\mathbf{J}^{-1}\mathbf{C}$ is not negligible by construction. v_t and $\mathbf{v}_m$ denote ITA and MTA thrust noise; u_t and $\mathbf{u}_m$ denote the relevant thrusts; K_t and $\mathbf{K}_m$ the voltage-to-force scale factors.

D. Sensor dynamics and noise

GOCE scientific payloads are employed as position and acceleration sensors.

1) The Gravity Gradiometer will provide 6-axes acceleration measurements.
2) Two GPS receivers will provide COM position and velocity, the raw measurements for LORF quaternion estimation.
3) In addition, two Star Tracker Units (STU), in cold redundancy, will provide the attitude quaternion $\mathcal{Q}$.

For details on measurement equations and on gradiometer dynamics see [7]. Gradiometer noise is typical of servo-accelerometers with a PSD reaching a minimum inside the MBW $\mathcal{F}_1$, while increasing toward lower and higher frequencies (see Fig. 2).

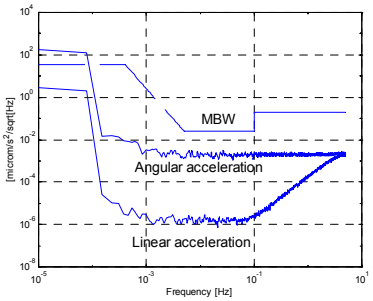

Fig. 2. PSD of the gradiometer noise for linear and angular measures compared to DFAC acceleration requirement (TABLE 1).

Denote linear and angular acceleration 3D vectors with $\mathbf{a}_h$, $h=l,a$ and the corresponding measures, in acceleration units, with $\mathbf{y}_h$. In view of the Embedded Model and according to Fig. 2, gradiometer errors are decomposed into a low-frequency component $\mathbf{b}_h$, including bias and drift, and a high-frequency one $\mathbf{v}_h$, including white and f^2 noise. The measurement equation, sampled at DFAC time unit $T=0.1$ s, follows:

$$\mathbf{y}_h(i)=\mathbf{y}_{0h}(i)+\mathbf{v}_h(i)+\mathbf{b}_h(i),\ \mathbf{y}_{0h}(i)=\mathbf{F}_h\cdot\mathbf{a}_h(i), \quad (9)$$

where $\mathbf{F}_h$ denotes either a linear dynamic operator or the relevant Z-transform.

Although GPS measurements are provided at a lower rate (1 Hz) and delayed, they will be treated at the DFAC rate $f_c=10$ Hz. Rate and delay will be managed by the reference generator in charge of estimating the LORF quaternion $\mathcal{Q}_O$. Position and velocity measures $\mathbf{y}_r$ and $\mathbf{y}_v$ will be affected by noise vectors $\mathbf{v}_r$ and $\mathbf{v}_v$ as follows:

$$\mathbf{y}_r(i)=\mathbf{r}(i)+\mathbf{v}_r(i),\ \ \mathbf{y}_v(i)=\mathbf{v}(i)+\mathbf{v}_v(i). \quad (10)$$

Let $\mathcal{Q}_S(i)$ the measured quaternion provided by the active STU. Misalignment of $\mathcal{Q}_S$ with respect to the inertial attitude quaternion $\mathcal{Q}$ is accounted for by an instrument quaternion $\mathcal{Q}_{Sv}$, which is the composition of calibration errors and noise, as follows:

$$\mathcal{Q}_S(i)=\mathcal{Q}(i)\otimes\mathcal{Q}_{Sv}(i). \quad (11)$$

The attitude vector $\mathbf{q}$ with respect to LORF, below 1 mrad from DFAC requirements, can be extracted by means of the LORF quaternion $\mathcal{Q}_O$, as follows

$$\mathcal{Q}_O^*(i)\otimes\mathcal{Q}_S(i)\simeq\left[1\quad\left[\mathbf{q}(i)+\mathbf{v}_S(i)\right]^T/2\right]^T, \quad (12)$$

where $\mathbf{v}_s(i)$ is the STU noise and the symbols $\otimes$ and $*$ denote quaternion product and conjugate.

IV. Embedded Model for Digital Control

A. Introduction

The DFAC was designed and implemented using a method inspired by [4]. The key point is the construction of the *Embedded Model* (EM), to be included as the core of control algorithms. The EM is realized in three steps:

1) The *controllable/observable* part of the fine model is simplified by neglecting: (i) cross-coupling and non-linear terms, treated as unknown/known disturbances, (ii) high-frequency dynamics, whose effect, if not excited by commands, remains within target tolerance.
2) A suitable class $\mathcal{D}$ of unknown, observable disturbances is synthesized, capable of encompassing the expected disturbance realization to be counteracted within target tolerance. Class complexity is derived from experimental/simulated PSD as in Fig. 1.
3) The EM is completed with analytic models (not treated here) of unmodelled dynamics, together with their uncertainties, not to be embedded but driving the tuning of closed-loop eigenvalues, to be refined against simulator and plant.

Control strategies can be viewed as tunable interfaces of the EM toward plant measurements and commands.

1) The Command Law (CL) computes the commands as a combination of tracking errors and estimated disturbances to be rejected.
2) The Measurement Law (ML), driven by the measures, estimates the noise so as to update realizations of $\mathcal{D}$.

The ensemble EM and ML (the part estimating the driving noise) can be viewed as a state predictor.

B. Requirements and performance variables

DFAC requirements in TABLE 1 correspond to zero

reference trajectories for the performance variables below:

$$\underline{\mathbf{a}}_l = \underline{\mathbf{a}}_a = 0,\ \ \underline{\mathbf{q}} = 0,\ \ \underline{\Delta\boldsymbol{\omega}} = 0\,, \tag{13}$$

where: (i) $\mathbf{a}_l$ and $\mathbf{a}_a$ denote residual linear and angular accelerations, (ii) $\mathbf{q}$ and $\Delta\boldsymbol{\omega}^T = \begin{vmatrix}\omega_x & \omega_O - \omega_y & \omega_z\end{vmatrix}$ denote attitude and rate with respect to LORF.

Reference trajectory (13) enlightens a key difference:

1) COM motion has to be free falling, i.e. only forced by gravity, with no requirement to COM position $\mathbf{r}$ and velocity $\mathbf{v}$. Accordingly, only the non-gravitational acceleration $\mathbf{a}_l$ will be controlled to zero from the gradiometer measurement $\mathbf{y}_l$ (*drag-free control*).
2) Attitude control, taking advantage of gradiometer measurements $\mathbf{y}_a$, can be hierarchically decomposed into *drag-free control* and *attitude control*, capable of bounding attitude and rate effects due to the residual angular acceleration $\mathbf{a}_q$, which is defined as the sum of $\mathbf{a}_a$ and of the gradiometer drift $\mathbf{d}_q = -\mathbf{b}_a$ (see (9))

$$\mathbf{a}_q = \mathbf{a}_a + \mathbf{d}_q\,. \tag{14}$$

C. Controllable/observable dynamics decomposition

The EM (see Fig. 3) is a multivariable DT state equation from $n_u = 9$ command components in $\mathbf{u}^T = \begin{bmatrix} u_t \mid \mathbf{u}_m^T \end{bmatrix}$ to $n_y = 15$ output variables arranged in the vector

$$\begin{aligned}&\mathbf{y}_0^T(i) = \begin{bmatrix}\mathbf{y}_{0r}^T(i) & \mathbf{y}_{0v}^T(i) & \mathbf{y}_{0q}^T(i) & \mathbf{y}_{0l}^T(i) & \mathbf{y}_{0a}^T(i)\end{bmatrix},\\ &\mathbf{y}_{0r} = \mathbf{r},\ \mathbf{y}_{0v} = \mathbf{v},\ \mathbf{y}_{0q} = \mathbf{q}.\end{aligned} \tag{15}$$

A 1st decomposition principle, *coordinate decomposition,* allows separating EM into six dynamics:

1) three separate *orbit dynamics* $\mathbf{P}_{r,c}$, one for each COM coordinate $c = x, y, z$, driven by the residual acceleration $\mathbf{a}_l$ and gravity $\mathbf{g}$,
2) three separate *attitude dynamics* $\mathbf{P}_{q,c}$, one for each Euler angle $c = x, y, z$, driven by the residual acceleration $\mathbf{a}_a$.

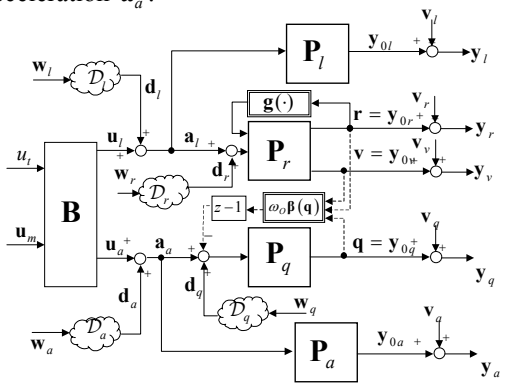

Fig. 3. Block diagram of the Embedded Model

Decomposition results from the following assumptions.

1) *Kinematic cross-coupling* between attitude angles (dashed lines in Fig. 3), which are non linera functions of the EM state variables, are treated as *known input signals*, so as to linearize the EM state equations. The same applies to *ITA cross-coupling*, part of the matrix $\mathbf{B}$ in (8).
2) All other cross-coupling terms, like gyro torques in Euler dynamics, are treated as unknown disturbances.

A 2nd decomposition principle, *hierarchical decomposition,* follows from sub-Section B.

1) *Drag-free control* will be based on restricted *thruster-to-gradiometer* dynamics $\mathbf{P}_l$ and $\mathbf{P}_a$, whose output variables are the the gradiometer error-free measures $\mathbf{y}_{0l}$ and $\mathbf{y}_{0a}$. The relevant DT model expressed as a Z-transform holds:

$$\begin{bmatrix}\mathbf{y}_{0l}\\ \mathbf{y}_{0a}\end{bmatrix}(z) = \begin{bmatrix}\mathbf{P}_l & 0\\ 0 & \mathbf{P}_a\end{bmatrix}\left(\mathbf{B}\begin{bmatrix}u_t\\ \mathbf{u}_m\end{bmatrix}(z) + \begin{bmatrix}\mathbf{d}_l\\ \mathbf{d}_a\end{bmatrix}(z)\right), \tag{16}$$

where $\mathbf{P}_l(z) = \mathbf{P}_a(z) = \mathrm{diag}\left\{z^{-1}, z^{-1}, z^{-1}\right\}$ accounts for gradiometer dynamics, $\mathbf{d}_l$ and $\mathbf{d}_a$ account for non-gravitational accelerations and unmodelled cross-coupling components.

2) *Attitude control* and *LORF estimation* will be based on the attitude and orbit dynamics $\mathbf{P}_r(z)$ and $\mathbf{P}_q(z)$, which are driven by the residual accelerations corrupted by gradiometer drift and gravity perturbations. By omitting z, they can be written as:

$$\begin{bmatrix}\mathbf{r}\\ \mathbf{q}\end{bmatrix} = \begin{bmatrix}\mathbf{P}_r & 0\\ 0 & \mathbf{P}_q\end{bmatrix}\left(\begin{bmatrix}\mathbf{a}_l\\ \mathbf{a}_a\end{bmatrix} + \begin{bmatrix}\mathbf{d}_r\\ \mathbf{d}_q\end{bmatrix} - \begin{bmatrix}(\mathbf{R}_O\mathbf{R})^T\mathbf{g}(\mathbf{r})\\ (z-1)\boldsymbol{\beta}(\mathbf{q})\omega_O\end{bmatrix}\right), \tag{17}$$

$$\begin{aligned}\mathbf{P}_r(z) &= T^2\,\mathrm{diag}\left\{(z-1)^{-2}, (z-1)^{-2}, (z-1)^{-2}\right\}\mathbf{R}_O\mathbf{R}\\ \mathbf{P}_q(z) &= T^2\,\mathrm{diag}\left\{(z-1)^{-2}, (z-1)^{-2}, (z-1)^{-2}\right\}\end{aligned} \tag{18}$$

As already said, nonlinear terms in (17) describing the gravity acceleration $\mathbf{g}(\mathbf{r})$ and the kinematic cross-coupling $\boldsymbol{\beta}(\mathbf{q})\omega_O$ are treated as *known input signals*, while $\mathbf{d}_r$ accounts for gradiometer drift.

D. Disturbance class dynamics

Four disturbance classes $\mathcal{D}_{h,c}$, $h = a, l, r, q$ per each coordinate axis $c = x, y, z$ are to be modelled:

1) non-gravitational accelerations $\mathbf{d}_l$ and $\mathbf{d}_a$ including thruster noise, unmodelled cross-couplings, drag, magnetic and gravity-gradient accelerations,
2) gradiometer drift accelerations $\mathbf{d}_r$ and $\mathbf{d}_q$.

Disturbance classes $\mathcal{D}_{h,c}$ are linear combinations of random drifts driven by white noise vectors $\mathbf{w}_{h,c}$:

$$\begin{aligned}&d_{h,c}(z) = \mathbf{D}_{h,c}^{(n)}(z)\mathbf{w}_{h,c}(z),\ \dim\mathbf{w}_{h,c} = (n+1),\\ &\mathbf{D}_{h,c}^{(n)}(z) = \begin{bmatrix}1 & (z-1)^{-1} & (z-1)^{-2} & \ldots & (z-1)^{-n}\end{bmatrix}.\\ &\mathcal{E}\left\{\mathbf{w}_{h,c}(i)\right\} = 0,\ \mathcal{E}\left\{\mathbf{w}_{h,c}(i)\mathbf{w}_{h,c}^T(j)\right\} = W_{h,c}^2\delta_{ij} < \infty,\end{aligned} \tag{19}$$

By choosing n in (19) and the resulting $S_{h,c}^2(f)$ so as to envelope the experimental PSD, the actual disturbance realizations are expected to be fully included in $\mathcal{D}_{h,c}$. For instance, as the drag and thruster noise PSD rolls of at -20 dB/dec, $n = 1$ would be adequate to $\mathbf{d}_l$ and $\mathbf{d}_a$. However,

to be conservative, $n=2$ was adopted. For what concerns gravity perturbations $\mathbf{d}_r$, as Kaula's rule [8] suggests their PSD to roll off at -40 dB/dec. $n=2$ was adopted.

E. Measurement equations

Measurement equations express discrepancy between plant measures and EM output variables. By arranging the measures in the vector $\mathbf{y}(i)$ as follows:

$$\mathbf{y}^T(i)=\begin{bmatrix}\mathbf{y}_r^T(i) & \mathbf{y}_v^T(i) & \mathbf{y}_q^T(i) & \mathbf{y}_l^T(i) & \mathbf{y}_a^T(i)\end{bmatrix}, \quad (20)$$

a generic measurement equation reads as:

$$\mathbf{y}_h(i)=\mathbf{y}_{0h}(i)+\mathbf{v}_h(i)+\partial\mathbf{P}_h(\mathbf{y}_{0h}(\mathbf{u},\mathbf{w}_h)), \quad (21)$$

where $h=r,v,q,l,a$, $\mathbf{v}_h$ is the measurement noise defined in Section III, except for the attitude noise $\mathbf{v}_q(i)$, and $\partial\mathbf{P}_h$ is the unmodelled dynamics operator.

The attitude noise vector $\mathbf{v}_q(i)$ is the composition of the STU noise $\mathbf{v}_S$ as in (12) and of the LORF estimation error, which results from replacing $\mathcal{Q}_O$ with the estimate $\hat{\mathcal{Q}}_O$ in (12). Upon definition of the LORF estimation error as

$$\mathcal{E}_O=\mathcal{Q}_O^*\otimes\hat{\mathcal{Q}}_O\simeq\begin{bmatrix}1 & \hat{\mathbf{e}}_O^T/2\end{bmatrix}^T, \quad (22)$$

the attitude measurement equation converts into

$$\hat{\mathcal{Q}}_O^*\otimes\mathcal{Q}_S\simeq\begin{bmatrix}1 & \left(\mathbf{q}+\mathbf{v}_q\right)^T/2\end{bmatrix}^T,\ \mathbf{v}_q(i)=\mathbf{v}_S(i)-\hat{\mathbf{e}}_O(i). \quad (23)$$

V. Digital Control

As already said, digital control follows from the EM in the form of a Command Law and a Measurement Law.

A. Control Law (CL)

Hierarchical decomposition implies to have three sets of CL, two of them allowing COM and attitude drag-free control and a third one allowing attitude control.

Drag-free CL follows from (16) by expressing residual accelerations as command/disturbance composition

$$\begin{bmatrix}a_{lx}\\ \mathbf{a}_{l,yz}\\ \mathbf{a}_a\end{bmatrix}(i)=\begin{bmatrix}B_{tx} & 0\\ \mathbf{B}_{t,yz} & \mathbf{B}_{m,yz}\\ \mathbf{B}_{ta} & \mathbf{B}_{ma}\end{bmatrix}\begin{bmatrix}u_t\\ \mathbf{u}_m\end{bmatrix}(i)+\begin{bmatrix}d_{lx}\\ \mathbf{d}_{l,yz}\\ \mathbf{d}_a\end{bmatrix}(i), \quad (24)$$

and forcing them to zero according to (13). In (24), $\mathbf{B}$ has been decomposed to separate ITA and MTA commands as well as linear and angular accelerations. By introducing the disturbance estimates to be provided by the EM and the ML (see Section B below), the drag-free CL follows:

$$u_t(i)=-\hat{d}_{lx}(i)/B_{tx}$$
$$\begin{bmatrix}\mathbf{B}_{m,yz}\\ \mathbf{B}_{ma}\end{bmatrix}\mathbf{u}_m(i)=-\begin{bmatrix}\mathbf{B}_{t,yz}\\ \mathbf{B}_{ta}\end{bmatrix}u_t(i)-\begin{bmatrix}\hat{\mathbf{d}}_{l,yz}\\ \hat{\mathbf{d}}_a\end{bmatrix}(i)+\begin{bmatrix}0\\ \mathbf{C}_q\end{bmatrix}(i). \quad (25)$$

The role of the attitude command term $\mathbf{C}_q$ in (25) is to cancel the non observable gradiometer drift from the acceleration estimate $\hat{\mathbf{d}}_a(i)$. The second equation in (25) is a set of five equations in eight unknowns, the entries of the MTA thrusts vector $\mathbf{u}_m(i)$, which can be solved through a pseudo-inverse $\mathbf{B}_m^{-1}$ capable of minimizing the average thrust in agreement with saving policies (not treated here).

According to (13), attitude control must force to zero attitude and rate and at the same time cancel gradiometer drift $\mathbf{d}_q$ from acceleration estimates $\hat{\mathbf{d}}_a$. This implies a CL which is the composition of attitude and rate tracking errors $-\hat{\mathbf{q}}$ and $-\Delta\hat{\boldsymbol{\omega}}$, as well as of drift estimates $\hat{\mathbf{d}}_q$:

$$\mathbf{C}_q(i)=-\mathbf{K}_1\hat{\mathbf{q}}(i)-\mathbf{K}_2\Delta\hat{\boldsymbol{\omega}}(i)-\hat{\mathbf{d}}_q(i), \quad (26)$$

where, exploiting coordinate decomposition, the feedback gain matrices $\mathbf{K}_1,\mathbf{K}_2$ become diagonal and their values depend on the closed-loop attitude eigenvalue set Λ_{kq}.

B. Measurement Law (ML)

Four white noise vectors, driving the actual realization of each disturbance class $\mathcal{D}_h$, have to be estimated from plant measures $\mathbf{y}(i)$. According to hierarchical decomposition, the 15 sensor measures have been decoupled as follows.

1) $\mathbf{w}_l$ and $\mathbf{w}_a$, driving the unknown non-gravitational disturbances $\mathbf{d}_l$ and $\mathbf{d}_a$, are estimated from linear and angular gradiometer measurements $\mathbf{y}_l$ and $\mathbf{y}_a$ (ML1).
2) $\mathbf{w}_q$, driving the angular gradiometer drift $\mathbf{d}_q$, is estimated from attitude measurements $\mathbf{y}_q$ (ML2).
3) $\mathbf{w}_r$, driving the unmodelled gravity perturbations $\mathbf{d}_r$, is estimated from COM position and velocity measurements $\mathbf{y}_r$ and $\mathbf{y}_v$ (ML3). Orbit dynamics in (17) together with ML2, providing the LORF estimate $\hat{\mathcal{Q}}_O$, plays the role of the reference attitude generator.

Let ML1 be restricted to angular dynamics. A similar ML applies to COM dynamics. ML1 is obtained by considering the EM made by the series $\mathbf{P}_{a,c}\cdot\mathbf{D}_{a,c}^{(2)}$ of the disturbance dynamics $\mathbf{D}_{a,c}^{(2)}$ and of the controllable dynamics $\mathbf{P}_{a,c}$, where $c=x,y,z$ stands for coordinate decomposition. The series is observable from $y_{a,c}$ and holds:

$$\mathbf{P}_{a,c}(z)\cdot\mathbf{D}_{a,c}^{(2)}(z)=z^{-1}\begin{bmatrix}1 & \left(z-1\right)^{-1} & \left(z-1\right)^{-2}\end{bmatrix}. \quad (27)$$

The corresponding ML can be easily shown to be a static feedback of the error $\hat{e}_{ya,c}=y_{a,c}-\hat{y}_{a,c}$ as in (28):

$$\hat{\mathbf{w}}_{a,c}(z)=\begin{bmatrix}\hat{w}_{a0,c}^T & \hat{w}_{a1,c}^T & \hat{w}_{a2,c}^T\end{bmatrix}^T=\mathbf{L}_{a,c}\hat{e}_{ya,c}(z), \quad (28)$$

since $\dim\mathbf{w}_{a,c}=3$ equals the order of the series in (27). Combination of (27) and (28) yields the observer equation:

$$\hat{y}_{a,c}(z)=\mathbf{V}_{oa,c}(z)y_{a,c}(z)+\left[1-\mathbf{V}_{oa,c}(z)\right]\mathbf{P}_{a,c}(z)u_{a,c}(z), \quad (29)$$

where the state observer linear dynamics $\mathbf{V}_{oa,c}$ holds:

$$\mathbf{V}_{oa,c}(z)=\left[1+\mathbf{P}_{a,c}\mathbf{D}_{a,c}^{(2)}\mathbf{L}_{a,c}\right]^{-1}\mathbf{P}_{a,c}\mathbf{D}_{a,c}^{(2)}\mathbf{L}_{a,c}. \quad (30)$$

The vector $\mathbf{L}_{a,c}$ contains three non zero gains for tuning the state observer eigenvalues $\Lambda_{a,c}$.

Differently than ML1, ML2 can not be a static feedback law as in (28), as the series of dynamics operators

$$\mathbf{P}_{q,c}(z)\cdot\mathbf{D}_{q,c}^{(2)}(z)=T^2\left(z-1\right)^{-2}\begin{bmatrix}1 & \left(z-1\right)^{-1} & \left(z-1\right)^{-2}\end{bmatrix} \quad (31)$$

has an order greater than $\dim \mathbf{w}_{q,c} = 3$. The least order dynamic ML can be shown to be 1st order and equal to:

$$\hat{\mathbf{w}}_{q,c}(z) = \begin{bmatrix} \hat{w}_{q0,c} \\ \hat{w}_{q1,c} \\ \hat{w}_{q2,c} \end{bmatrix} = \mathbf{L}_{q,c} \begin{bmatrix} 1 \\ \dfrac{1}{z-(1-\beta)} \end{bmatrix} \hat{e}_{yq,c}(z), \quad (32)$$

where $\hat{e}_{yq,c} = y_{q,c} - \hat{y}_{q,c}$ is the attitude angle output error, $\mathbf{L}_{q,c}$ is a 3×2 constant-gain matrix with four non-zero gains and $1-\beta$ is the open-loop eigenvalue of the ML, to be tuned together with $\mathbf{L}_{q,c}$ to obtain observer eigenvalues $\Lambda_{q,c}$. According to (32) and omitting z for brevity, a similar equation to (29) holds for the attitude observer:

$$\hat{y}_{q,c} = \mathbf{V}_{oq,c} y_{q,c} + \mathbf{S}_{oq,c} \left(\mathbf{P}_{a,c} \hat{a}_{a,c} - (z-1) \beta_c (\hat{\mathbf{y}}_q) \hat{\omega}_O \right) \quad (33)$$

where $\mathbf{V}_{oq,c}(z)$, similar to (30), is the attitude observer dynamics, while $\mathbf{S}_{oq,c} = 1 - \mathbf{V}_{oq,c}$ is the relevant sensitivity.

Finally, because the dynamic operator series $\mathbf{P}_{r,c} \cdot \mathbf{D}_{r,c}^{(2)}$ has an order $n = 4$ greater than $\dim \mathbf{w}_{r,c} = 3$, ML3 would be of the dynamic type as ML2. However, a static ML was employed, because two different measurements $y_{r,c}$ and $y_{v,c}$ are available for each coordinate axis $c = x, y, z$.

C. Robust stability and eigenvalue tuning

Internal stability. The closed-loop system made by the DFAC laws and by the EM, free of modeling errors, or in other words assuming $\partial \mathbf{P}_h(\cdot) = 0$ in (21), can be shown to be internally stable, if and only if the eigenvalue sets $\Lambda_l, \Lambda_a, \Lambda_q$ and Λ_{cq} lie inside the unit disk.

Stability recovery. When the measurement vectors $\mathbf{y}_h(i)$ derive from the plant, the assumptions guaranteeing internal stability cease to be valid because of the modeling errors $\partial \mathbf{P}_h$. Their effects spill through plant measures $\mathbf{y}$ by making the estimation error $\hat{\mathbf{e}} = \mathbf{y}_0 - \hat{\mathbf{y}}$ to be command-dependent via a complex/uncertain dynamic operator $\hat{\mathbf{e}} = \mathbf{E}(\mathbf{y}_0(\mathbf{u}, \mathbf{w}))$. For instance, by restricting the angular acceleration to a single axis $c = x, y, z$, the estimation error $\hat{e}_{a,c} = y_{0a,c} - \hat{y}_{a,c}$ can be rewritten as:

$$\hat{e}_{a,c}(z) = \mathbf{E}_{a,c}\left(y_{0a,c}\left(u_{a,c}, \mathbf{w}_{a,c} \right) \right) = \mathbf{V}_{oa,c}(z) \partial \mathbf{P}_{a,c}\left(y_{0a,c} \right), . \quad (34)$$

Fortunately, as (34) shows, the ML has an intrinsic capability of bounding the closed-loop effect of the unmodelled dynamics $\partial \mathbf{P}_{a,c}(\cdot)$ by means of the observer dynamics $\mathbf{V}_{oa,c}(z)$, so as to fully recover closed-loop stability. According to [4], the key way is to assign the eigenvalue set $\Lambda_{a,c}$ to the unit disk in order to sufficiently bound the effect of $\mathbf{E}_{a,c}$ on the error $\hat{e}_{a,c}$. Although analytic conditions can be derived from simplified models of $\partial \mathbf{P}_h(\cdot)$, complexity and uncertainty suggest refining observer eigenvalues against simulated fine models prior to in-field set-up and test.

VI. Simulated Results

Fig. 4 shows the PSD of the linear accelerations under worst-case spacecraft/environment conditions. They are compared to the target bound defined in TABLE 1.

Target accuracy is met with good margin from MBW to $f_c/2$. The critical accuracy that appears at low frequencies for cross-axis accelerations, is the price to be paid for thrust level minimization. Fig. 5 shows the PSD of attitude q_x, angular rate $\Delta\omega_x$ and of the residual angular acceleration $a_{a,x}$ with respect to the relevant DFAC requirements. Further results, time plots and details about DFAC and simulation will be provided at the conference presentation.

DFAC has been integrated into end-to-end GOCE simulator at Alenia Spazio premises, providing same performances.

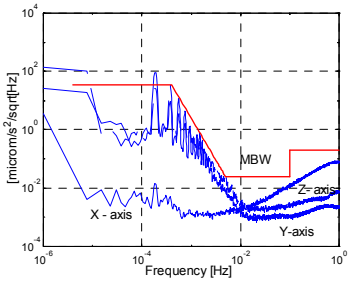

Fig. 4. PSD of the residual linear accelerations compared to target bound. Ordinate: $\mu m/s^2/\sqrt{Hz}$.

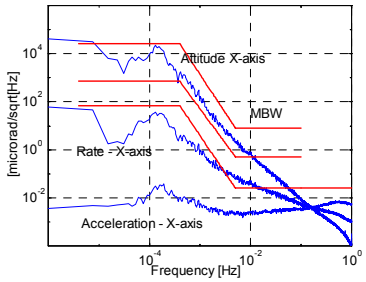

Fig. 5. PSD of attitude $[\mu rad/\sqrt{Hz}]$, rate $[\mu rad/s/\sqrt{Hz}]$ and residual acceleration $[\mu rad/s^2/\sqrt{Hz}]$ relevant to $c = x$ Euler angle compared to DFAC requirements.

References

[1] J.A. Johannessen and M. Aguirre-Martinez "Gravity Field and Steady-State Ocean Circulation Mission", *The Four Candidate Earth Explorer Core Missions*. ESA SP-1233, July 1999

[2] O. Montenbruck and E. Gill, *Satellite Orbits – Models, Methods, Applications*. Springer, 2000.

[3] B. Bertotti and P. Farinella, *Physics of the Earth and the Solar System*. Kluwer Academic, 1990.

[4] F. Donati and M. Vallauri, "Guaranteed control of 'almost-linear' plants". *IEEE Trans. on Autom. Control* 29 (1), 34-41.

[5] E. Canuto, F. Musso and D. Andreis "Embedded model control: application to electro-valves", submitted to *IEEE Med. Control Conf.*, Cyprus, 2005.

[6] E. Canuto and A. Rolino "Multi-input digital frequency stabilization of monolithic lasers", *Automatica*, 40(12), 2004, p. 2139-2147.

[7] E. Canuto, B. Bona, G. Calafiore and M. Indri, "Drag-free control for the European satellite GOCE. Part I: modelling", In: *Proc. 41st IEEE Conf. Dec. and Control,* 2002, pp.1269-1274.

[8] W. M. Kaula, *Theory of Satellite Geodesy*, Blaisdell Publishing Co, Waltham, Massachusetts, 1966.